

Depositional morphotypes and characterization of silica diagenesis in Ypresian-Priabonian gypsiferous carbonates, Gafsa, Southern Tunisia

Mohsen Henchiri (✉ mohsen.henchiri@fsg.mu.tn)

University of Gafsa

Rim Zammali

University of Gafsa

Khawla Abid

University of Gafsa

Mohamed Khalil Zidi

University of Gafsa

Walid Ben Ahmed

University of Gafsa

Research Article

Keywords: Gypsiferous carbonates, Silica diagenesis, Anhydrite, Nodules, Gafsa basin, Tunisia

Posted Date: June 29th, 2022

DOI: <https://doi.org/10.21203/rs.3.rs-1724854/v1>

License: © ⓘ This work is licensed under a Creative Commons Attribution 4.0 International License. [Read Full License](#)

Abstract

Silica diagenetic features have been recognized in the Ypressian – Priabonian gypsiferous carbonates of Kef Edour Member in Gafsa basin, southern Tunisia. These rocks host a broad range of nodular features including anhydrite / gypsum, nodules and silica geodes. Three types of silica geodes have been recognized based on colour, form, chemical and mineralogical composition. A zoned texture characterizes most of geodes, with (1) a rim, 34 cm thick, composed of mixed microquartz and (2) length-slow chalcedony and (3) euhedral Megaquartz lining the inner cavity of the nodule. XRD analysis reveals that the quartz is the only silica phase present in most samples. The other silica forms (opaline group = opal-A, opal-C, opal-CT) are undetectable with XRD. FTIR and ^{29}Si MAS NMR analyses confirm the presence of diagenetic hydroxylated silica forms (silanol sites with two bridging oxygen sites $Q_2(-(\text{O})_2\text{Si}(\text{OH})_2)$) interpreted as amorphous opaline precursors of the quartz. Other non-siliceous groups have been detected, such as SO_4 (sulphate evaporites) CO_3 (calcium and magnesium carbonates), and confirmed by petrographic observations. In Mg-rich and gypsiferous host sediments, silica diagenesis tends to proceed discontinuously. During early silicification, pore fluid chemistry ($\text{pH} < 9$) tolerates silica replacements and the development of the microcrystalline and fibrous form of quartz, whereas this silica replacement is slowed down or curtailed later in the innermost parts of anhydrite nodules due pore fluid chemistry (pH values > 9) allowing the development of euhedral silica form by force of crystallization supported by its crystallinity degree and its low specific surface area and ultramicroporosity that make it the most mineralogically competent and the most chemically resistant in such environments. Silica supply could be derived ultimately from (1) minor volcanogenic/hydrothermal venting contributions during early diagenetic stages, and (2) diagenesis of the extraformational and overlying detrital quartz and clay-rich sediments.

Introduction

Silica diagenesis in evaporitic environments has long been recognized as replacement events with leading to diagenetic silica nodules production (quartz geodes). Several papers (Hayes, 1964; Folk and Pittman, 1971; siedlecka, 1972; Chowns & Elkins, 1974; Tucker, 1976; Milliken, 1979; Salameh and Schneider, 1980; Elorza & Rodriguez-Lazaro, 1984; Maliva, 1987; Alonso-Zarza *et al.*, 2002), all discuss the existence of inclusions of precursor evaporites in quartz crystals and argue the replacement origin of quartz. This replacement approach is widely adopted without assessment of the diagenetic potential and the susceptibility to silicification of the replaced evaporitic sediments. However, relatively few papers (e.g., Chafetz & Zhang, 1998, Henchiri *et al.* 2015) provide data about the causal relationships between silica diagenesis and its bearing sediment (sulphate and Mg-rich sediments). More concerns are pertained to the origin and the significance of some silica growth fabrics associated with evaporites (concretionary and botryoidal silica as well as well-developed pyramidal terminated megaquartz crystals) which are so far poorly understood, and question like “can these silica fabrics be evaluated as a simple replacement phenomenon?” are still posed with considerable controversy over the origin of these fabrics (i.e. euhedral megaquartz) occurring in evaporites, halides and Mg-rich environments (Table 1).

The purposes of the present study are (1) sedimentological study of silica nodules (geodes) hosted in gypsiferous carbonate rocks, (2) physico-chemical characterization of silica diagenesis (3) discussing the susceptibility of the replaced host rocks (evaporites) to silicification, (4) the significance of the association of some silica fabrics with evaporites and (5) possible silica sources for silicification. This study is based on field and lab-based investigations using XRD, FTIR, ^{29}Si MAS NMR, SEM-EDX and petrographic microscopy..

Geological Setting

The host sedimentary rocks of the randomly disseminated silica and gypsum/anhydrite nodules are the gypsiferous carbonate sequence of the Upper Metlaoui Formation, which is of Ypressian-Priabonian age localized in the region of Gafsa (Figs. 1a). They were deposited on marine phosphorites of Lower Ypressian age in Gafsa pull-apart basin. Burolet (1956), during his stratigraphic classification, used the term Metlaoui Formation for > 50 m of phosphate marl and dolomitic and gypsiferous limestone exposed at Thelja, west of Metlaoui region (Fig. 1b). The rocks in the present study were later included in the Kef Eddour Member by Chaabani (1995). The Kef Eddour Member is overlain by Oligocene to Pliocene continental deposits (Sehib, Beglia and Segui Formations). This Member is well developed in the Mzinda and Jellabia areas (Henchiri, 2002, 2007). It is ~ 18.7 m thick in the study area (Oued El Khasfa) and thinning towards the eastern parts of the basin. The sediments are white to yellow and chalky, with local phosphatic ooids, and gypsum/anhydrite nodules that were weathered to produce abundant voids and porous textures now mainly filled with various types of silica nodules.

Materials And Methods

Measured sections and methodical sampling were carried out in 6 outcrops and 4 phosphate quarries. Approximately 86 silica, anhydrite/gypsum and carbonate nodular fabrics were obtained, sorted and described. A Phillips XL20 scanning electron microscope (SEM) was used to study the texture and petrography of the types of silica nodules (geodes) present. Additional information on their composition (Na, Mg, Si, Fe, Al, K and Ca) was obtained by energy dispersive X-ray analysis (EDX) using a Cameca SX51 electron microprobe with 15 kV acceleration voltage, 20 nA current intensity, and a 10- μm beam diameter. The samples were analysed by X-ray diffraction using a Siemens D500 diffractometer (CuK α radiation, 45 kV, 40 mA) to confirm the mineralogy and the crystallinity of the mineral phases. These analyses were supplemented with thin sections of polished slabs of silica nodules that were prepared for transmitted light petrography. FTIR spectroscopy of the different silica forms were recorded using Perkin-Elmer FTIR-Spectra-photometer in the mid-infrared region at room temperature. Each sample was pestle in an agate mortar, then sieved to less than 2.5 micron and mixing 1/100 weight with potassium bromide (KBr). FTIR results are collected from the spectral range of 350– 4000 cm^{-1} . Diffractograms and FTIR spectra were analyzed respectively with High-Score $^{\circ}$ and Opus $^{\circ}$ softwares for peak search.

Nuclear magnetic resonance spectroscopy is carried out on representative small slices taken from the most homogenous parts of quartz geode samples ground to a fine powder and tightly packed into the rotors of the probe. The instrument for MAS NMR (magic angle spinning nuclear magnetic resonance) spectra is a Bruker 300 MHz PM Ultra shield spectrometer in the laboratory of industrial chemistry of « l'Ecole Nationale d'Ingénieurs de Sfax, ENIS », with a

rotor with a diameter of 7 mm and spinning rate of 3 kHz and operating frequency of 79.5 MHz, with 5-min delay between the pulses for complete relaxation. Chemical shifts (coordination variation) were measured relative to the ^{29}Si resonance of tetramethylsilane for ^{29}Si NMR spectra. Half-width, peak height, peak area and chemical shift of the signals were determined by least squares curve fitting using Lorentzian functions in Mestrec NMR 3.2© software.

Results And Interpretations

Gypsiferous carbonate lithofacies and fabrics

These rocks are present as isolated nodules and thin laminae within non-evaporitic host sediments. In outcrop, these sediments (Fig. 2a, b) High porosity and locally important *in situ* brecciation and collapse structures are common sedimentary features, attributed partly to the volume reduction during the mineral transformation and in part to the dissolution of soluble salts by weathering. Some of these vuggy and collapse structures can deliver, after weathering, nodules made up of gypsum/anhydrite or microquartz and length-fast chalcedony. Locally they display large scale teepee structure (Fig. 2c) with yellowish, powdery appearance due to the partial conversion of saccharoidal gypsum into microcrystalline anhydrite, in response to the present hot and arid climate (Fig. 2d, f). Broad range of nodular features can be identified (Fig. 3), including scattered nodules, and massive, chicken-wire and enterolithic structures that may form continuous but undulating planar bodies. It's assumed that the evaporites had already transformed into anhydrite, and may in fact be rehydrating to gypsum in the meteoric realm.

Fabrics and petrography of silica nodules

Three types of silica nodules (Table 2), which are present mainly in the upper parts of Kef Eddour Member, have a spherical to subspherical shape and range in size from 5 cm to > 10 cm in diameter. They are usually found as erosional remnants where the Eocene sediments were subaerially exposed. In buried sediments (Jellabia quarry), however, nodules are commonly interconnected and concentrated along individual horizons, with different degrees of silicification and exhibit replacement of the host sediment and dissolution of the anhydrite.

Nodule types

Type A: These nodules (Fig. 4a, b) were found as scattered erosion remnants in Mzinda, Jallabia and Oued el Khasfa and in buried sediments. They are up to 80 % of silica nodules and they have spherical to subspherical shape with 5 cm to 10 cm in diameter. They generally show brown reddish and dark colours suggesting an active organic component as indicated by Ulmer-Scholle (1993). The outer part of the nodule show unreplaced evaporite-rich carbonates speckles that escaped silicification. The silicified groundmasses comprise microcrystalline quartz and zebraic chalcedony in the outer zone, chalcedony in the middle zone and megaquartz crystals with euhedral terminations of those lining the central cavity. These megacrystalline crystals range in length from 20 to 90 μm .

Type B: They present 10 to 20 % of silica nodules (Fig. 4c). They are most abundant in Mzinda, Jallabia and Oued el Khasfa mainly as erosion remnants. In buried sediments the recognition of these nodules is difficult due to their external crust yellow colour making them confused with the encasing Gypsiferous carbonates. They have spherical to subspherical, oblate and slightly elongated 5 cm to 10 cm in diameter and 8 cm to 15 cm in length. The quartz groundmasses are bluish transparent to limpid with clear and non-altered vitreous luster. The meacrystalline quartz is the prevailing silica variety with abundant centimeter-long well-faceted euhedral single or doubly terminated megaquartz crystals.

Type C: These nodules are minor (5 to 10 % of silica nodules) (Fig. 4d, e) and belong ultimately to inner basin localities (Mzinda and Jallabia). They have spherical shape with frequent lower flattened bases and 4 cm to 8 cm in diameter. Silica groundmasses show an occluded central cavity with megaquartz crystals with yellow brownish color indicative of abundance of limonite Fe-oxide minerals interpreted as being of infiltration origin. The outer surface may display impression of marine calcareous and siliceous sponges. (Fig. 4f) Also, it's notable the progressive transition from the chalcedonic silica zone to megaquartz crystals zone with vitreous luster and lamellar aspect.

Texture

An average texture of silica nodules was inferred from the different observations made. From the margin to the centre of each nodule (Fig. 4g), a zoned texture was observed with a carbonate crust, 5 mm thick, composed of partially silicified micrite and dolomicrite that includes claystone and detrital grains from the host sediment; (1) a rim, 34 cm thick, composed of mixed microquartz (Fig. 5a) and (2) length-slow chalcedony showing, in places, concentric growth bands and coatings. These varieties of silica grade inward, by a gradual increase in the crystal size, into granular to pseudocubic to (3) euhedral megaquartz, which, generally, lined the inner cavity of the nodule (Fig. 5b). The euhedral quartz crystal-lined cavity, in several cases, shows unreplaced solid inclusions made up of anhydrite relics (Fig. 5c), halite, dolomite, calcite, oxides and hydroxides (goethite) (Fig. 5d, e), as well as primary heterogeneous fluid inclusions (Fig. 5f) composed of two phase aqueous (L+V) inclusions, with a liquid (L) and a vapour bubble (V).

Mineralogy

XRD analyses

XRD analyses of silica from different parts of the nodule (Fig. 6a) show that quartz (easy to diagnosis compared to other silica polymorphs) is the only silica polymorph present in most samples. The quartz has a crystallinity index (Murata & Norman, 1976, Smith, 1998) of 45. The three amorphous forms of opaline group (opal-A, opal-C and opal-CT) are not detected in the diffractograms at 2.5\AA for opal-A and 4\AA (22,2 [20]) for opal-CT. However, accessory minerals including some small relict patches of unreplaced anhydrite, gypsum calcite, barite, dolomite and halite that escaped replacement, and minor K-feldspar and plagioclase are detected in some samples. The clay fraction is marked by faint amount (0.1 %) of illite and kaolinite distributed preferentially in outer silicified

parts of the nodule. Amorphous opaline group (with short-range order in quartz geodes) are sometimes difficult to detect or to diagnose using conventional techniques such as powder X-ray diffraction (applicable only to mineral phases with long-range order). These mineral phases are mostly in trace amounts under the detection limits of this apparatus and they are not detected in the diffractograms.

Infrared spectroscopy

Peak search for mineral identification of silica phases and other minerals included within the silica groundmasses of quartz geodes was carried out on a transmittance of the infrared wave length within the area covering 400 – 4000 cm^{-1} (Fig. 6b). Quartz phase occurring in geodes is characterized by three peak ranges corresponding to Si-O asymmetrical bending vibrations in the area of 461- 464 and 509 - 514 cm^{-1} ; peaks in the range of 690-695 cm^{-1} correspond to Si-O symmetrical bending vibrations, while peaks at 795-800 cm^{-1} are attributed to Si-O symmetrical stretching vibrations. Peaks at 555 cm^{-1} and 562 cm^{-1} represent a vibration band of Si-O belonging to SiO_4 tetrahedra (Schmidt and Fröhlich, 2011). O-Si-O bending vibration is represented by the 480 cm^{-1} band. Peaks at 1100 and 790 cm^{-1} are belong to antisymmetric and symmetric Si-O-Si stretching respectively (Adamo et al. 2010). The peak at 1600 and 1920 cm^{-1} is related to the vibration of free (adsorbed) H_2O and OH stretching. The Peaks at 1077 and 456 cm^{-1} are often missing or under-represented in other spectra by the isolated bands at 776 and 795 cm^{-1} , which are indicators of quartz (Povarennykh 1978). Peaks at 1145 and 1120 cm^{-1} are attributed to a vibration band of SO_4 . Carbonate vibration bands are at 1427 and 874 cm^{-1} . Organic compounds are represented by the peaks at 1274 and 1448 cm^{-1} and a shoulder at 1710 cm^{-1} .

^{29}Si MAS NMR

Some mineral phases are difficult to detect using XRD and conventional optical means (SEM and TEM) because of their low abundance; many phases are present in trace amounts below the detection limits of those instruments. In the samples studied, the opaline precursor of the microcrystalline quartz is below the detection limits of the X-ray diffractometer. Nevertheless, the microspherical shape of some weakly certified relics is attributed to probable traces of former opal-CT lepispheres. ^{29}Si MAS NMR analysis provides a viable alternative to XRD for mineralogical identification (Stebbins, 1988; Spearing & Stebbins, 1989; Stebbins & Farnan, 1989). This method was used to determine if the diagenetic microquartz in the quartz geode was derived from an opal-CT precursor. The ^{29}Si MAS NMR spectra of microcrystalline quartz and chalcedony show the well defined peak of normal quartz (Fig. 6c) microcrystalline quartz with siloxane sites with four bridging oxygen atoms at -102.52 p.p.m Q_4 ($-\text{O}_3\text{SiO}-$) (Stebbins, 1987). Another peak at 111 p.p.m. (silanol sites with two bridging oxygen sites Q_2 ($-(\text{O})_2\text{Si}(\text{OH})_2$), related to an amorphous silica form (Sherriff & Hartman, 1985). The latter is interpreted as an opaline silica precursor that is under-represented and masked. A small but broad resonance assigned to silanol sites with three bridging oxygen atoms at -94.03 p.p.m, resonance Q_3 ($-(\text{O})_3\text{Si}(\text{OH})$).

Chemical composition

Chemical elements were detected qualitatively using SEM-based EDAX microprobe (for example, Fig. 5d, e) and are presented in Table 2. Some chemical elements have variable composition while passing from the outer to the inner zone of the nodule such as Mg, Ca, Na, K, S, Cl, P. Mg and Ca are ascribed to the gypsumiferous carbonates that form an outer crust. Na, K and Cl are attributed to halide inclusions (NaCl and KCl) trapped by silica groundmasses during replacement. P is interpreted as being of organic matter origin as mentioned above in the type-A nodules (for example, Chang et al., 2020).

Discussion

Silica diagenesis in evaporitic environment

Origin of diagenetic silica nodules

Maliva (1987) suggested that quartz crystallizes after dissolution of the anhydrite nodule in the host rock, producing a nodule that consists of solid quartz, with, in some examples, a euhedral crystal-lined central cavity. During silica replacement of the sulphates, the rate of silica precipitation is controlled by anhydrite dissolution and pore fluid chemistry (pH) (Fig. 7) (Demangeon, 1966; Perthuisot et al., 1978; Stamataki, 1989). In the samples studied (Fig. 8), silica replacement began in the outer parts of the anhydrite nodules and proceeded inward displacively towards the centre of the nodules. The replacement of the outer parts of the nodules resulted in a decrease of pore water salinity and pH that enabled silica precipitation (for example Touray and Cheghan, 1984; Maliva and Siever, 1988). The remaining anhydrite was dissolved later after the decrease in pH and dilution of the pore fluids that previously had curtailed inward growth of silica. This situation led to the creation of a central cavity in the nodule, in which other minerals can precipitate. This process implies that the silica replacement was basically controlled by the chemistry of the pore fluids during diagenesis (Henchiri et al., 2015). Moreover, the outer parts of the anhydrite, which are the most altered and leached and implying more dilute conditions (cf. Alonso-Zarza et al., 2002), had lower pH values (> 7 and < 9) that permitted silica precipitation in the form of rims. In contrast, the pH was highly alkaline (> 9) in the innermost parts of the anhydrite nodules. The high pH did not allow the continuation of anhydrite groundmass silicification, and this pH-controlled process was probably responsible for the “geode” features (Tucker, 1976; Maliva, 1987). This model also explains why silicification (or certification) of the anhydrite nodules always proceeded inward and not outward. It is feasible that silica precipitation, in this case, could have been a continuous steady process if the dissolution (or the shifting of alkalinity) of the innermost anhydrite proceeded as fast as the silica-rich fluid was supplied.

According to Schmidt et al. (2001), Pore fluid pH can strongly affect the ratio (Si-O-Si/Si-OH) (i.e. $Q_4/(Q_3+Q_2)$) through silica-water surface chemistry and silica solubility and precipitation (Knauss & Wolery, 1988; Brady & Walther, 1989; Dove & Elston, 1992; House & Orr, 1992; Berger et al., 1994; Dove, 1994; Mazer & Walther, 1994). The ^{29}Si spectrum intensity is known to decrease with increasing pH (Carroll et al., 2002). Silica dissolution - precipitation may be pH controlled: the quartz geodes may have formed in alkaline high pH conditions that originated from the electrolyte (Berger et al., 1994) and sodium chloride

solutions (Dove, 1994) in ambient fluids and evaporites. The resulting silicified groundmasses are predominantly related to pore-water silica supersaturation and the force of crystallization (as defined by Maliva and Siever (1988)) during their formation.

The dense form of the silica rind appears to have precluded any silica diffusion after the pore fluid chemistry-induced barrier to inward growth of the silica. On the other hand, siliceous phases have formed as later mineral phases in the cavities that were produced by the late innermost anhydrite dissolution. This poses the following questions that can be deciphered only by extensive field and laboratory work: why did silica cementation not occlude the entire cavity (without alkalinity constraints) and thus produce silicified bodies that resemble chert nodules (i.e. 90-95% chertified)? Was growth of the chert nodule aborted? Gomez-Alday *et al.* (2002) posed similar questions when considering the origin of quartz geodes in northern Spain.

The direct silicification of sulphate evaporite nodules into silica nodules, like those resulting from carbonate nodules chertification (characterized by high silica replacements percentage exceeding 98 %), seems to be constrained by the chemical barrier existing within evaporitic nodules preventing the entire silicification of nodule. Only partial replacements can take place leading to geodic nodules by creation of a “diagenetic closed system” (Tucker, 1976; Henchiri and Shimi, 2006) in which, silica inward growth is curtailed.

Pore fluid chemical barrier

Practically, pore water pH can affect strongly the silica precipitation, which, in our case, can be explained by its clear tendency to be pH-controlled during replacement of sulphate evaporites (gypsum/anhydrite nodules). Sulphates and chlorides-rich (NaCl) inclusions and salty connate fluids in the innermost parts of evaporite nodule are responsible for silica curtailed growth and the generation of “geode” feature. Alkaline high-pH conditions in innermost parts of evaporite nodule are interpreted to have resulted largely from the electrolyte (Berger *et al.*, 1994) and sodium chloride solutions (Dove, 1994) included within evaporite bodies in different proportions. These components can provide locally highly concentrated alkaline solutions with pH >9 that can nullify or make silicification difficult. That is what makes differences in silicification patterns and fabrics between the outer and inner parts of some nodules.

Origin of megaquartz variety related to evaporites

As explained above, the incomplete silicification of evaporite nodules can lead to that silica is a difficult mineral to form in high-pH environment chemistry (with some exceptions, i.e. Lake Magadi and Lake Bogoria: microbial-induced silicification (Renault *et al.*, 2002)); thereby the megaquartz crystals, which represent the last silica phase precipitated in direct contact with evaporite phase, were developed probably before the total dissolution of remnant evaporites as indicated by the richness of trapped evaporite inclusions in quartz. The palissade-like megaquartz crystals observed in the inner cavity of geodes may not necessarily express a “diagenetic relief” of silicification but it’s rather interpreted as a sign of constrained process, because silica-rich diagenetic fluids in sulphate or Mg-rich environment tend to precipitate the well-developed, single or double terminated euhedral megaquartz variety. Higher alkalinity degrees implies euhedral megaquartz with large faceted crystal variety indicative of low growth rates (Siever, 1962 ; Ernst and Clavert, 1969 ; Maliva and Siever, 1988). In literature, it has been found that the slowest growing crystals are the crystals more likely to be the largest ones. Similar situations with unanswered questions about euhedral shape of quartz are reviewed in Demangeon, (1966); Friedman & Shukla, (1979); Touray & Chegham, (1984); Fabricius, (1984); Maliva, (1987); Eilon *et al.*, (1988); Ulmer-Scholle, (1993); Chafetz & Zhang, (1998); Alonso-Zarza, (2002); El Khoriby, (2005). However, the close association of euhedral megaquartz variety to evaporite or Mg-rich environments suggests that this silica habit variety is the most competent in such environments.

The relationship between silica diagenesis and evaporites is not yet well enough understood. Folk and Pittman (1971) and Gomez-Alday *et al.* (2002) have reported the well-crystallized euhedral forms of quartz in relation to evaporite to low silica concentrations supply during silicification. Similar situations with non-resolved questions about euhedral shape of quartz in relation to evaporite are reviewed in Table 1. However, the explanation of the close association of euhedral megaquartz variety with evaporite and/or Mg-rich environments is found in the physical properties of this silica habit (Henchiri *et al.*, 2015) such as its crystallinity degree (Murata & Norman, 1976) and its low specific surface area and ultramicroporosity (Bustillo *et al.*, 1993) that make it the most mineralogically competent and the most chemically resistant in such environments.

Silica supply

Clocchiati and Sassi, (1972) and Beji-Sassi *et al.*, (2001) reported traces of Paleocene-Eocene volcanic/ hydrothermal venting activity (glassy inclusions in quartz crystals) in Gafsa Basin within the phosphorites that underlie the studied sediments near the Oued El Khasfa. This volcanogenic / hydrothermal contribution of silica supply for silica nodule formation, especially during the early diagenetic stages of silicification of the anhydrite nodules, is of major significance. Although dissolved and reworked, most silica of volcanic origin is rapidly altered and transformed into authigenic zeolites (clinoptilolite), as suggested by Sassi & Jacob (1972) and Henchiri (2007).

Silica-rich diagenetic fluid can be supplied through clay mineral diagenesis (i.e. transformation of smectite to hydrous mica or illite according to two possible reaction stoichiometries) as suggested by Towe (1962), Helling (1978), Boles & Franks (1979) and Dietzel, (2000). The host sediments are clay-poor with only minor amounts of smectite and kaolinite. Thus, the provenance of soluble silica is thought more likely to be derived, during late diagenesis, from the pressure solution of silt and sand grains, or from feldspar and mica dissolution in the Oligo-Miocene continental sand, silt and clay-rich formations (Sehib, Beglia and Segui) that overlie the host sediments. Silica-rich fluids moved downwards and reached the host sediments through repeated silica dissolution, transport and reprecipitation (Makhlouf *et al.*, 2015).

Conclusion

Detailed sedimentological and geochemical analysis of silica and evaporite nodules of the Eocene Kef Eddour Member near Sehib in Tunisia has led to the following conclusions:

- 1) Silicification of anhydrite nodules is an early diagenetic process that seems to be pH- controlled. The innermost parts of the nodule preserved an alkaline character due to higher pH values that curtailed the progressive inward silicification. Even after dissolution of the anhydrite remains, the pH barrier persisted.
- 2) Quartz crystal length is under immediate control of the alkalinity of pore water of replaced mineral phase and the ambient water chemistry and the availability of sufficient and diffusive silica supply. The dilute conditions in the outer parts of evaporite nodule with high silica concentration imply the precipitation of quartzine-lutecite (fibrous microquartz and chalcedony), whereas the high-pH alkalinity in the innermost parts of nodule with low silica concentration implies the precipitation of megaquartz crystals.
- 3) The close association of euhedral megaquartz variety with evaporitic environments can be explained by the physical properties of this silica habit such as its crystallinity degree and its low specific surface area and ultramicroporosity that make it the most competent and resistant in such environments.
- 4) Silicification of the gypsum-anhydrite nodules is blocked after the installation of a closed system in the innermost parts where the evaporitic material exists but cannot be silicified, in contrast with the already known and accepted interpretations without contesting or excluding them.
- 5) The silica-rich diagenetic fluids could have been derived ultimately from the extraformational sandy and clay-rich beds that overlie the studied sediments during late diagenesis, with minor contributions from volcanogenic and sources in an early stage of diagenesis.

Declarations

Author contributions

All authors contributed to the study conception and design. Material preparation, data collection and analysis were performed by Mohsen Henchiri, Khawla Abid, Mohamed Khalil Zidi and Walid Ben Ahmed. The first draft of the manuscript was written by Mohsen Henchiri. All authors read and approved the final manuscript.

Data availability

No additional data available (common).

Declaration of competing interest

The authors declare that they have no known competing financial interests or personal relationships that could have appeared to influence the work reported in this paper. References

References

1. Adamo I, Ghisoli C, Caucia F (2010) A contribution to the study of FTIR spectra of opals, Neues Jahrbuch Für Mineralogie - Abhandlungen. 187 63–68. doi:10.1127/0077-7757/2010/0161.
2. Alonso-Zarza, M.A., Sánchez-Moya, Y., Bustillo, M.A., Sopena A., Delgado, A. 2002. Silicification and dolomitization of anhydrite nodules in argillaceous terrestrial deposits: an example of meteoric-dominated diagenesis from the Triassic of central Spain. *Sedimentology* 9, 303-312.
3. Baker, G. 1957. Microcrystalline quartz crystals in brown coal, Victoria. *American Mineralogist* 31, 22-30.
4. Beji-Sassi, A., Laridhi-Ouzaa, N., Zaier, A., Clocchiatti, R. 2001. Paleocene-Early Eocene alkaline volcanic activity in Tunisia phosphatic sediments. Comparison with cretaceous magmatism and geodynamic significance. *Les journées de l'ETAP 2001* pp. 47-58.
5. Berger, G., Cadore, E., Schott, J., Dove, P.M. 1994. Dissolution rate of quartz in lead and sodium electrolyte solution between 25 and 300 °C: Effect of nature of surface complexes and reaction affinity. *Geochimica Cosmochimica Acta* 58, 541-552.
6. Bertolino, M., Cattaneo-Vietti, R., Pansini, M., Santini, C., Bavestrello, G., 2017. Siliceous sponge spicule dissolution: in field experimental evidences from temperate and tropical waters. *Estuarine Coastal and Shelf Science*, 184:46-53.
7. Black, W. W. 1949. **An occurrence of authigenic feldspar and quartz in Yoredale limestones** *Geological Magazine* 86, 129.
8. Boles, R.J., Franks, G.S. 1979. Clay diagenesis in Wilcox sandstones of southwest Texas: Implications of smectite diagenesis on sandstones cementation. *Journal of Sedimentary Petrology* 49, 55-70.
9. Bonte, A. 1953. Sur la genèse des quartz bipyramidés. *Comptes Rendues Scientifiques de la Société Géologique de France* 13 : 253.
10. Burolet, P.F. 1956. Contribution à l'étude stratigraphique de la Tunisie centrale. Ph.D. thesis, Université de Paris 350 pp.
11. Bustillo, M.A., Fort, R., Bustillo, M. 1993. Specific surface area and ultramicroporosity in polymorphs of silica. *European Journal of Mineralogy* 5, 1195-1204.
12. Chaabani, F. 1995. Dynamique de la partie orientale du bassin de Gafsa au Crétacé et au Paléogène : Etude minéralogique et géochimique de la série phosphatée éocène (Tunisie méridionale). Ph.D. Thesis. Université Tunis II, 428 pp.
13. Chafetz, H.S. Zhang, J. 1998. Authigenic euhedral megaquartz crystals in a quaternary dolomite. *Journal of Sedimentary Research* 68, 994-1000.
14. Chowns, T.M., Elkins, J.E. 1974. The origin of quartz geodes and cauliflower chert through the silicification of anhydrite nodules. *Journal of Sedimentary Petrology* 44, 885-903.
15. Clocchiatti, R. and Sassi, S. 1972. Découverte de témoin d'un volcanisme paléocène à éocène dans le bassin phosphaté de Metlaoui (Tunisie méridionale) *C.R. Acad. Sci., Paris.* 274, 513-517.

16. Conley, D.J, Frings, P.J., Guillaume, F., et al., 2017. Biosilicification Drives a Decline of Dissolved Si in the Oceans through Geologic Time. *Frontiers in Marine Science*, 4:397.
17. De Master, D.J., 2003. The diagenesis of biogenic silica: Chemical transformations occurring in the water column, seabed, and crust. *Treatise on geochemistry*, 7:87-98.
18. De Wever, P, Dumitrica, P, Caulet, J.-P, Nigrini, C., Caridroit, M., 2001. Radiolarians in the Sedimentary Record. Gordon & Breach, London.
19. Demangeon, P. 1966. A propos des quartz authigènes des terrains salifères. *Bulletin de la Society Française de Minéralogie et de Cristallographie LXXXIX*, 484-487.
20. Dietzel M 2000. Dissolution of silicates and the stability of polysilicic acid. *Geochim Cosmochim Acta* 64(19):3275–3281
21. Dove, P.M. 1994. The dissolution kinetics of quartz in sodium chloride solutions at 25°C to 300 °C. *American Journal of Science* 294, 665-712.
22. Ehrlich H., 2011. Silica Biomineralization, Sponges, in: Reitner, J., Thiel, V. (Eds.), *Encyclopedia of Geobiology*. Springer, Dordrecht, pp. 1-12.
23. Eilon, G., Lang, B., Starinsky, A. Touret, J. 1988. A fluid inclusion investigation of cenomanian quartz geodes in Israel: a possible heliothermal effect. *Bulletin of Mineralogy* 111, 557-566.
24. El Khoriby, I.M. 2005. Origin of the gypsum-rich silica nodules, Moghra Formation, Northwest Qattara depression, Western Desert, Egypt. *Sedimentary Geology* 179, 205-220.
25. Elorza, J., Rodriguez-Lazaro, J. 1984. Late Cretaceous quartz geodes after anhydrite from Burgos, Spain. *Geological Magazine* 121, 107-113.
26. Fabricius, J. 1984. Formation temperature and chemistry of brine inclusions in euhedral quartz crystals from Permian Salt in the Danish Trough. *Bulletin of Mineralogy* 107, 203-216.
27. Folk, R.L., Pittman, J.S. 1971. Length-slow chalcedony: a new testament for vanished evaporites. *Journal of Sedimentary Petrology* 41, 1045-1058.
28. Friedman G., Shulka V. 1979 Significance of authigenic quartz euhedra after sulfates: Example from the Lockport Formation (Middle Silurian) of New York. *Journal of Sedimentary Petrology* 50, 1299-1304.
29. Gomez-Alday, J., Garcia-Garmilla, F., Elorza, J. 2002. Origin of quartz geodes from Lano and Tubilla del Agua sections (middle-upper Campanian, Basque-Cantabrian Basin, northern Spain) : isotopic differences during diagenetic processes. *Geological Journal* 37, 117-134.
30. Graetsch, H., Flörke, O.W. Miehe, G. 1985. The nature of water in chalcedony and opal-C from brazilian agate geodes. *Phys Chem Minerals* 12, 300–306 <https://doi.org/10.1007/BF00310343>
31. Hayes, J.B. 1964. **Geodes and concretions from the Mississippian Warsaw Formation, Keokuk region, Iowa, Illinois, Missouri** *Journal of Sedimentary Research*. 34, 123 - 133.
32. Heling, D. 1978. Diagenesis of illite in argillaceous sediments of the Rhinegraben. *Clay Mineralogy* 13, 211-219.
33. Henchiri, M. 2002. Le phosphate siliceux de Sehib : caractérisation minéralogique, granulochimique et séparation des gangues stériles, *Mémoire de Faculté des Sciences de Tunis.*, 107pp.
34. Henchiri, M., Abidi, R. & Jemmali, N. 2015. Large euhedral quartz crystals in the Triassic dolomites and evaporites of central Tunisia: implications for silica diagenesis in sulphate-rich and high-Mg environments. *Arabian Journal of Geosciences* 8, 8899–8910 <https://doi.org/10.1007/s12517-015-1788-5>
35. Henchiri, M., Slim-S'Himi, N., 2006. Silicification of sulphate evaporites and their carbonate replacements in Eocene marine sediments, Tunisia: two diagenetic trends. *Sedimentology* 53, 1135–1159. doi:10.1111/j.1365-3091.2006.00806.x.
36. Kehew A.E. 2001. *Applied chemical hydrogeology*. Prentice Hall, New Jersey, 368 pp
37. Makhoulouf, I.M., Tarawneh, K., Moumani, K. et al. 2015. Recognition of quartz geodes in the Upper Cretaceous Wadi Umm Ghudran Formation, Ras En Naqab, South Jordan. *Arabian Journal of Geosciences* 8, 1535–1547. <https://doi.org/10.1007/s12517-014-1281-6>.
38. Maliva, R.G. 1987. Quartz geodes: Early diagenetic chertified anhydrite nodules related to dolomitization. *Journal of Sedimentary Petrology* 57, 1054-1059.
39. Manning-Berg, A.R., Kah, L.C., 2017. Proterozoic microbial mats and their constraints on environments of silicification. *Geobiology*, 15:469-483.
40. Manning-Berg, A.R., Wood, R.S., Williford, K.H., Czaja, A.D., Kah, L.C., 2019. The taphonomy of Proterozoic microbial mats and implications for early diagenetic silicification. *Geosciences*, 9:40.
41. Milliken, L.K. 1979. The silicified evaporite syndrom, two aspects of silicification history of former evaporite nodules from southern kentucky and northern Tennessee. *Journal of Sedimentary Petrology* 49, 245-256.
42. Molenaar, N., de Jong, A.F.M. 1987. Authigenic quartz and albite in Devonian limestone: origin and significance. *Sedimentology* 34, 623-640.
43. Murata, K.J., Norman, M.B. 1976. An index of crystallinity of quartz. *American Journal of Science* 276, 1120-1130.
44. Noble, J.P.A., Van Stempvoort, D.R. 1989. **Early burial quartz authigenesis in Silurian platform carbonates, New Brunswick, Canada** *Journal of Sedimentary Research*. 59, 65 - 76.
45. Perthuisot, V., Guilhaumou N., Touray, J.C. 1978. Les inclusion fluids hypersalines et gazeuses des quartz et dolomites du Trias évaporitique Nord-Tunisien. *Essai d'interpretation géodynamique*. *Bulletin de la Société géologique de France* 20, 145-155.
46. Renaut, R.W., Jones, B., Tiercelin J.J., 2002. Rapid in situ silicification of microbes at Loburu hot springs, Lake Bogoria, Kenya Rift Valley. *Sedimentology*, 45:1083-1103.
47. Richter, D.K. 1972. Authigenic quartz preserving skeletal material. *Sedimentology* 19, 211-218.
48. Salameh, E., Schneider, W. 1980. Silica geodes in Upper Cretaceous dolomites, Jordan. Influence of calcareous skeletal debris in early diagenetic precipitation of silica *Neues Jahrbuch Geologie und Paleontologie* 3, 185-192.

49. Sassi, S., Jacob, C. 1972. Découverte de la clinoptilolite dans le bassin phosphaté de Métlouï (Tunisie). Comptes Rendues de l'Académie des Sciences. Paris 274, 1128-1131.
50. Schmidt P, Fröhlich F (2011) Temperature dependent crystallographic transformations in chalcedony, SiO₂, assessed in mid infrared spectroscopy, Spectrochimica Acta - Part A: Molecular and Biomolecular Spectroscopy. 78 1476–1481. doi:10.1016/j.saa.2011.01.036.
51. Siedlecka, A. 1972. Length-slow chalcedony and relics of sulfates-evidence of evaporitic environments in the Upper Carboniferous and Permian beds of bear island, Svalbard. Journal of Sedimentary Petrology 42, 812-816.
52. Smith, D.K., 1998. Opal, cristobalite, and tridymite: noncrystallinity versus crystallinity, nomenclature of the silica minerals and bibliography. Powder Diffraction, 13:2-19.
53. Stamatakis, M.G. 1989. **Authigenic silicates and silica polymorphs in the Miocene saline-alkaline deposits of the Karlovassi Basin, Samos, Greece.** Economic Geology 84, 788 - 798.
54. Tarr, W.A. 1929. Doubly terminated quartz crystals occurring in gypsum. American Mineralogist. 14, 19-25.
55. Touray, J. C. and Cheghan, A. 1984. Une paragenèse à anhydrite et barytine pseudomorphosée en quartz dans les filons métallifères de Sidi Lahcen (Maroc oriental). Bulletin de Minéralogie, 107, 813-815.
56. Towe, M.K. 1962. Clay mineral diagenesis as a possible source of silica cement in sedimentary rocks. Journal of Sedimentary Petrology 32, 26-28.
57. Tucker, M.E. 1976. Quartz replaces anhydrite nodules (Bristol Diamonds) from the Triassic of the Bristol District. Geological Magazine 113, 569-574.
58. Ulmer-Scholle, D.S., Scholle, P.A. Brady, P.V. 1993. Silicification of evaporites in permian (Guadalupian) Back-reef carbonates of the Delaware basin, West Texas and New Mexico. Journal of Sedimentary Research 63, 955-965.

Tables

Table 1

Silica diagenesis in various host rocks from the Silurian through the pleistocene

	location	Host rock lithology	diagenesis	reference
Late Pleistocene	Saudi Arabia-Jubayl	Dolomites and evaporites	Late/Meteoric	Chafetz and Zhang 1998
Miocene	Greece	Evaporites and halides	Late/ Meteoric	Stamatakis, 1989
Miocene	Australia	Coal	Late	Baker, 57
Tertiary	USA-Texas	Gypsum	Early/Marine	Tar, 1929
Cretaceous	Yoredal, England	Limestones/dolostones	Late/ Meteoric	Black, 1949
Triassic	Tunisia, Sidi Bouzid	Dolomite	Late/météorique	Henchiri et al. 2015
Triassic	France	Evaporites and chlorides	Late/ Meteoric	Bonte, 1953
Triassic	France	Evaporites and halides	Late/ Meteoric	Demangeon, 1966
Triassic	Tunisia-Le Kef	Evaporites and halides	Late/ Meteoric	Perthuisot et al., 1979
Permian	Denmark	Evaporites and halides	Early/Marine	Fabricius, 1984
Devonian	Belgium-Liège	Limestones/dolostones	Late/ Meteoric	Molenaar and de Jong, 1987
Devonian	Belgium-Liège	Limestones/dolostones	Late/Meteoric	Richter, 1972
Silurian	New York, USA	Evaporites and halides	Early/Marine	Friedman and Shulka, 1979
Silurian	Canada-N. brunswick	Carbonates	Late	Noble and Stempvoort 1989

Table 2

Characteristics of silica geodic nodules encountered in the study area.

Nodule types	Type A			Type B			Type C		
Size and shape	Spherical to subspherical 5 cm to > 10 cm in diameter			Spherical to subspherical, oblate and slightly elongated, 5 cm to 10 cm in diameter and 8 cm to 15 cm in length.			Spherical with frequent lower flattened cm to 8 cm in diameter		
Location	Oued el Khasfa, Jellabia and Mzinda			Oued el Khasfa, Jellabia and Mzinda			Jellabia and Mzinda		
Position	Erosional remnants and sediment-buried, upper Kef Eddour Member			Erosional remnants and sediment-buried, upper Kef Eddour Member			Erosional remnants and sediment-buried, upper Kef Eddour Member		
Chemical composition*	Si, Mg, Ca, Na, Al, S, P			Si, Ca, S, Al, Mg, Na, K			Si, Al, Na, Ca, Mg, S, K,		
Colour	Generally brown reddish and dark colours suggesting an active organic component			Bluish to limpid with clear and vitreous luster of quartz groundmasses			Yellow brownish colour due Fe-oxides limonites		
	Outer zone	Middle zone	Inner zone	Outer zone	Middle zone	Inner zone	Outer zone	Middle zone	Inner zone
Mineralogy	Microquartz, chalcedony, carbonates, eventual halides	Microquartz, chalcedony	Megaquartz, oxides, hydroxides, anhydrite, halides	Microquartz Carbonates, halides	Microquartz, halides	Megaquartz, oxides, hydroxides, anhydrite, halides	Microquartz, chalcedony, carbonates, eventual halides	Microquartz, chalcedony, halides	Megaquartz, oxides, hydroxides, anhydrite, halides
Texture	Microcrystalline quartz crystals of different dimensions	Concentric growths and coatings with inward gradual increase in the crystal size	granular to pseudocubic to palisade-like euhedral megaquartz	Microcrystalline quartz crystals of different dimensions	Fibrous with inward gradual increase in the crystal size	Large single or doubly terminated quartz crystals	Microcrystalline quartz crystals of different dimensions	Progressive transition from chalcedony to megaquartz	Megaquartz, oxides, hydroxides, anhydrite, halides
* : Chemical elements were detected qualitatively using SEM-based EDAX microprobe and are presented quantitatively from left to right in a decreasing order of abundance									

Figures

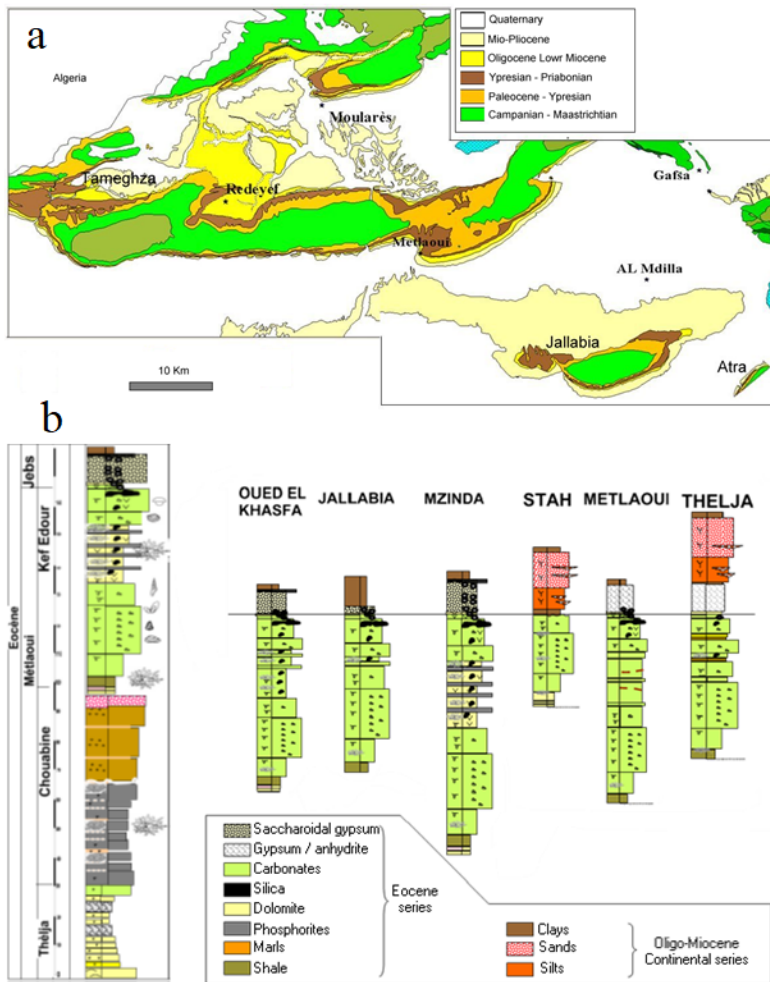


Figure 1
 (a) Location and geological map showing the main outcropping sedimentary rocks in the studied area. (b) lithostratigraphic sections showing the position of the studied sediments (Kef Eddour and Jebs Members).

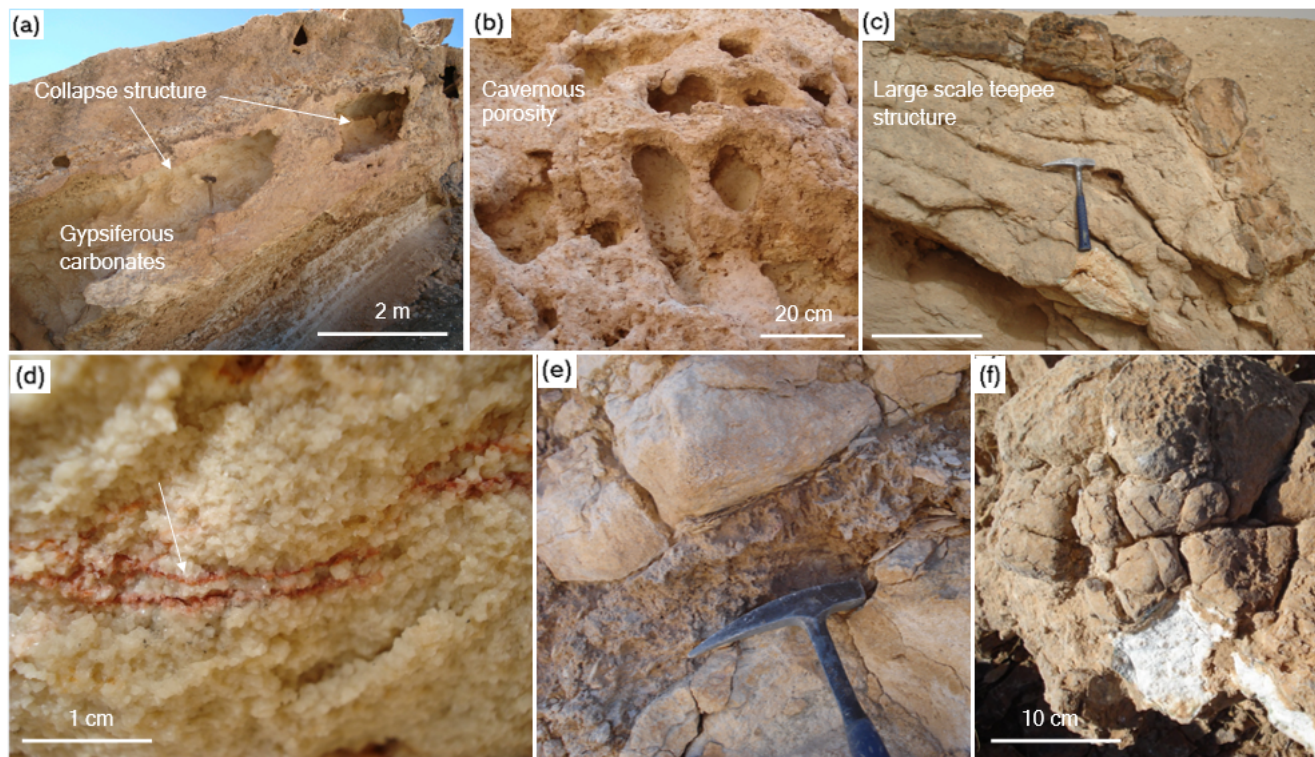


Figure 2
 Sedimentary aspects of gypsiferous carbonates of Kef Eddour Member. (a) Field view of the studied outcroppings of Kef Eddour Member near Oued El Khasfa with high porosity and locally important *in situ* brecciation and collapse structures. (b) Cavernous porosity resulting from leaching and weathering of soluble salts. (c) Large scale teepee structure. (d) Saccharoidal gypsum with infiltrated Fe-oxides. (e) friable gypsum with gypsiferous carbonate nodules. (f) Detail of gypsiferous carbonate nodule.

Nodular types	Field views	Description
		Preserved gypsum and anhydrite nodule encountered in the studied area with whitish to yellowish, powdery appearance due to the partial conversion of gypsum into microcrystalline anhydrite, in response to the present hot and arid climate.
		Gypsum and anhydrite nodule (1) with partially silicified carbonate crust (2). This crust probably formed at about the same time as the anhydrite nodule.
		10 cm-long, circular with two distinctive zones silica nodule; 1: chalcedony and microquartz, 2: agate (silicified carbonate crust)
		Regular quartz geode; 1: carbonate crust; 2: chalcedony and microquartz; 3: euhedral megaquartz; 4: euhedral quartz crystal-lined central cavity.

Figure 3

Inventory and description of nodular bodies encountered in the study area listed in the diagenesis evolutionary order.

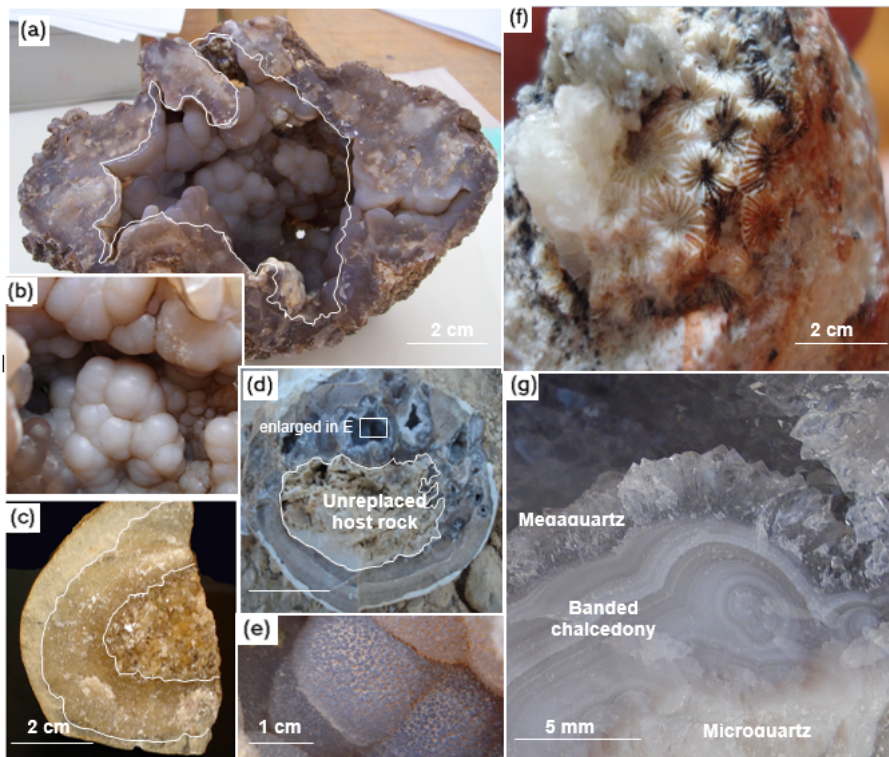


Figure 4
Types of silica nodules encountered in the study area. (a) Brown reddish silica nodule collected from Mzinda consisting of massive cryptocrystalline microquartz and lenth-slow chalcedony. The colour suggest an active organic component to this system, may be hydrocarbons. (b) Detail of (a) showing the concretionary and botryoidal growth of silica in the central cavity of the nodule. (c) Silica nodule showing an occluded central cavity with megaquartz crystals with yellowish color indicative of abundance of limonite minerals of pedogenic origin. (d) Silica nodule from Jellabia with unreplaced anhydrite. (e) Detail of (d) showing botryoidal growth habits with well-crystallised euhedral megaquartz terminations. (f) The outer surface of silica nodule showing the impression of siliceous sponges. (g) Progressive transition from microquartz through banded chalcedonic silica to palissadic megaquartz crystals lining the central cavity.



Figure 5

(a) Photomicrograph showing the outer zone of the nodule composed of microcrystalline quartz of different dimensions. Crossed Nichols. (b) Photomicrograph showing the middle zone of the nodule with inward gradual increase in the crystal size from the zebrachalcedony to the prismatic megaquartz. Crossed Nichols. (c) Photomicrograph showing the inner zone of the nodule composed of megacrystalline quartz with minor amount of anhydrite inclusions. (d) SEM photomicrographs of the inner zone of silica nodule (megacrystalline phase of quartz). (e) Microprobe spot analysis in microquartz showing the scarcity of halide inclusions (NaCl) (arrows) in this silica phase. (f) Microprobe spot analysis in megaquartz showing the abundance of halide inclusions (NaCl) (arrows) in this silica phase. (g) Fluid inclusions in the silica geodes with primary two phase (L+V) aqueous inclusions.

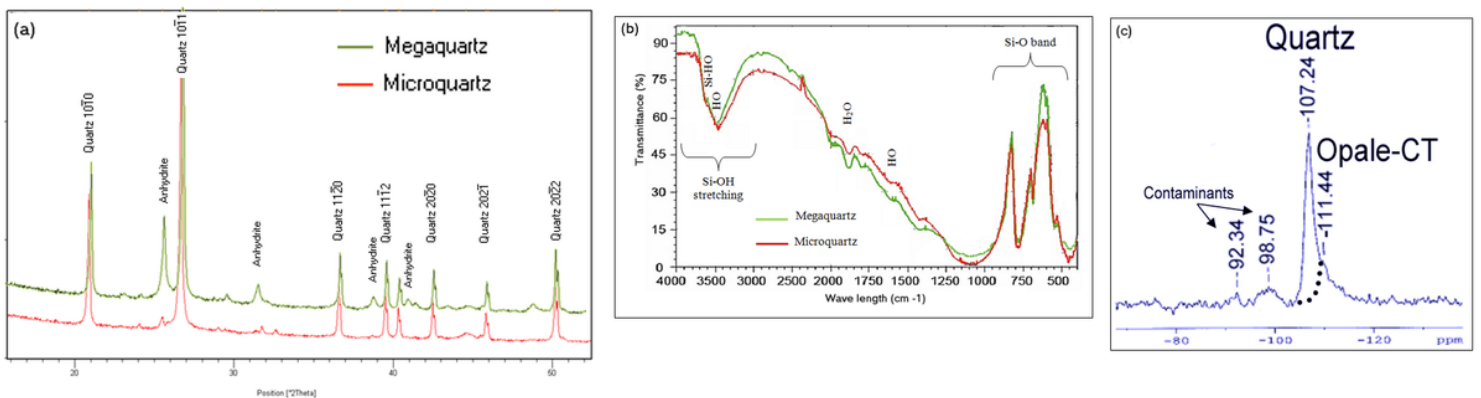


Figure 6

(a) XRD diffractograms of microquartz and megaquartz coming from silica geodes giving rise to the abundance of unreplaced anhydrite patches, as solid inclusions, in megaquartz crystals compared to microquartz. (b) FTIR spectra of Megaquartz and microquartz from silica geode. (c) ^{29}Si MAS NMR spectrum of quartz from silica geode.

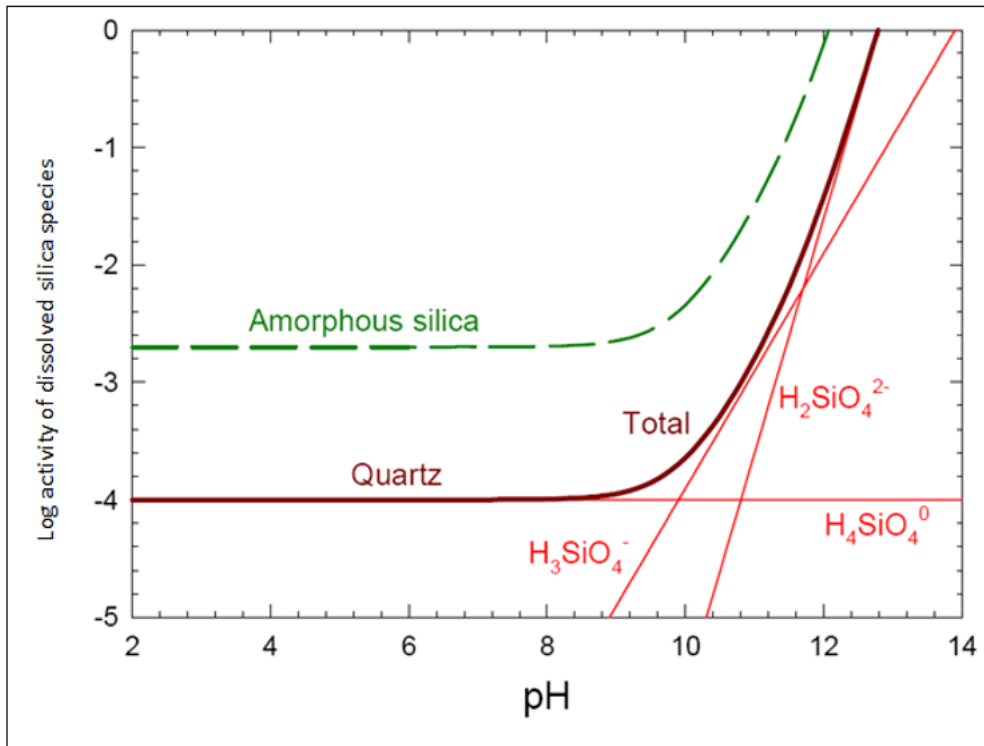


Figure 7

Relationship between silica solubility and pH of ambient fluids (Kehew 2001).

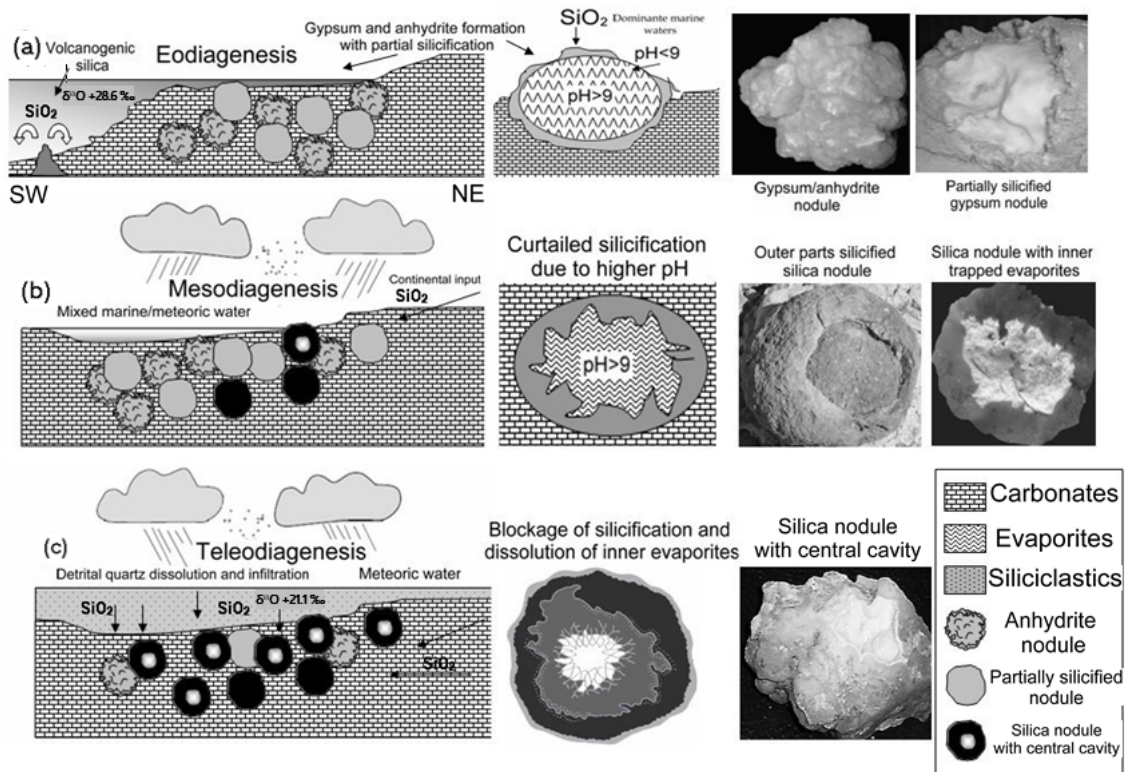


Figure 8

Schematic model summarizing the diagenesis of silica in Gypsiferous carbonates. (a) Early marine-dominated diagenetic stage with evaporite deposition and partial silicification of outer parts of nodules with volcanogenic silica. (b) Mesodiagenesis with mixed marine/meteoric diagenetic fluids with silica of continental provenance. The silicification of evaporite nodules is curtailed and becoming difficult due to the settlement of closed diagenetic system with low diffusive silica and high-pH alkalinity originated from trapped innermost evaporites and salty connate waters. (c) Late meteoric-dominated diagenesis characterized by the occurrence of the last silica phase (megaquartz crystals in the central cavity of the nodule) with dissolution of remnant evaporites. Silica is derived from the diagenetic reactions in the overlying siliciclastic continental formations responsible for the production of silica-rich circulating diagenetic fluids in fractures and diaclasses within host carbonates.